

Mutator Phenotypes Caused by Substitution at a Conserved Motif A Residue in Eukaryotic DNA Polymerase δ^*

Received for publication, September 19, 2005, and in revised form, December 8, 2005. Published, JBC Papers in Press, December 12, 2005, DOI 10.1074/jbc.M510245200

Ranga N. Venkatesan, Jessica J. Hsu, Nicole A. Lawrence¹, Bradley D. Preston, and Lawrence A. Loeb²

From the Department of Pathology, University of Washington, Seattle, Washington 98195-7705

Eukaryotic DNA polymerase (Pol) δ replicates chromosomal DNA and is also involved in DNA repair and genetic recombination. Motif A in Pol δ , containing the sequence DXXXLYPSI, includes a catalytically essential aspartic acid as well as other conserved residues of unknown function. Here, we used site-directed mutagenesis to create all 19 amino acid substitutions for the conserved Leu⁶¹² in Motif A of *Saccharomyces cerevisiae* Pol δ . We show that substitutions at Leu⁶¹² differentially affect viability, sensitivity to genotoxic agents, cell cycle progression, and replication fidelity. The eight viable mutants contained Ile, Val, Thr, Met, Phe, Lys, Asn, or Gly substitutions. Individual substitutions varied greatly in the nature and extent of attendant phenotypic deficiencies, exhibiting mutation rates that ranged from near wild type to a 37-fold increase. The L612M mutant exhibited a 7-fold elevation of mutation rate but essentially no detectable effects on other phenotypes monitored; the L612T mutant showed a nearly wild type mutation rate together with marked hypersensitivity to genotoxic agents; and the L612G and L612N strains exhibited relatively high mutation rates and severe deficits overall. We compare our results with those for homologous substitutions in prokaryotic and eukaryotic DNA polymerases and discuss the implications of our findings for the role of Leu⁶¹² in replication fidelity.

DNA-dependent DNA polymerases display a common catalytic mechanism and play a pivotal role in DNA replication, DNA repair, and genetic recombination (1). Sixteen different DNA polymerases have been identified in eukaryotic cells and are classified into four families (families A, B, Y, and X) based on sequence homology and presumed function (2). The eukaryotic enzymes in family B, comprised of DNA polymerases α , δ , ϵ , and ζ , are involved in DNA replication and also function in other DNA synthetic processes (3). One current replication model suggests that the DNA polymerase α -primase holoenzyme complex initiates *de novo* synthesis of primers, which are then extended by DNA polymerases (Pols)³ δ and ϵ (4–7). Pols δ and ϵ contain multiple conserved motifs; the N terminus harbors the 3' → 5' proofreading exonuclease and polymerase motifs, whereas the functions of the C terminus have not been established.

Pols δ and ϵ synthesize DNA with high fidelity and are highly processive upon interaction with proliferating cell nuclear antigen (8–10). Fidelity is achieved by the sequential, coordinated actions of the polym-

erase and 3' → 5' exonuclease proofreading domains. It has been estimated that Pols δ and ϵ incorporate approximately one noncomplementary nucleotide/10⁴–10⁶ nucleotides polymerized and that their exonuclease domains further enhance accuracy by 2–10-fold (5–7, 11). Structure-function studies of mutant DNA polymerases have led to identification of critical residues in conserved motifs A and B in the polymerase domain that affect fidelity of family A, family B, and family Y DNA polymerases (12–21). Results from several laboratories demonstrate that evolutionarily conserved amino acids in motifs A and B that form the nucleotide-binding pocket can tolerate substitutions (12–21). Substitution at motif A and B residues in both prokaryotic and eukaryotic DNA polymerases imparts a wide range of phenotypes, including reduced activity, compromised fidelity, altered substrate specificity, and DNA replication defects *in vivo* (13, 20, 22–24). However, replacement of any one of a catalytic triad of acidic amino acids, one in motif A and two in motif C, results in inactivation (25, 26).

In this work, we exploited the evolutionary homology in the catalytic domains of family A and family B DNA polymerases to create mutants of *Saccharomyces cerevisiae* Pol δ that increase mutation rates. We and others have previously shown that mutation at a conserved Ile in motif A of *Escherichia coli* DNA polymerase I and *Taq* DNA polymerase I alters fidelity (12, 15, 20, 21). Here, we created all 19 replacements for the homologous residue in yeast Pol δ and found that replacements at this position affect fidelity. We demonstrate that amino acid substitutions at Leu⁶¹² in *S. cerevisiae* motif A differentially affect viability, mutation rates, cell cycle progression, and sensitivity to genotoxic agents.

EXPERIMENTAL PROCEDURES

Yeast Strains—Standard recombinant DNA and yeast molecular genetic techniques, including growth media, were followed (27, 28). YGL27-3D (*MATa leu2 his3 ade2 trp1 lys2 ura3 pol3::KanMX* or *pol3::HIS3*), a kind gift of Gerard Faye (Institute Curie-Biologie), was the starting point for construction of strains used in this study (29). YGL27-3D harbors a lethal partial deletion of the chromosomal *POL3* gene; *POL3* function is provided by a wild type copy of the gene carried on the plasmid pGL310, derived from the *URA3* plasmid Ycp50-SUP11 (29). The entire chromosomal copy of *POL3* in YGL27-3D was replaced with a KanMX cassette to yield YGL27-*pol3* Δ .⁴ Similarly, we replaced the entire chromosomal copy of *POL3* in the strain BY4741 (*MATa his3-1 leu2 Δ met15 Δ ura3 Δ*) (ATCC, Manassas, VA) with a KanMX cassette to yield BY4741-*pol3* Δ ; *POL3* function is provided by a wild type copy of the gene carried on the plasmid YCplac33 (ATCC), which contains *URA3* selectable marker to obtain plasmid Ycplac33-*POL3*.

Generation of Pol δ Mutant Strains—To generate amino acid replacements at Leu⁶¹² of Pol δ , the plasmid YCplac111-*POL3* was utilized for site-directed mutagenesis using a QuikChange kit (Stratagene, San Diego, CA). YCplac111-*POL3* contains the wild type *POL3* gene

* This work was supported by National Institutes of Health Grants R01 CA102029 (to L. A. L.), R01 ES 09927 and R01 CA98243 (to B. D. P.), and P01 AG01751. The costs of publication of this article were defrayed in part by the payment of page charges. This article must therefore be hereby marked "advertisement" in accordance with 18 U.S.C. Section 1734 solely to indicate this fact.

¹ Present address: Abbott Laboratories, Abbott Park, IL 60064.

² To whom correspondence should be addressed. Tel.: 206-543-6015; Fax: 206-543-3967; E-mail: laloeb@u.washington.edu.

³ The abbreviations used are: Pol, DNA polymerase; FACS, fluorescence-activated cell sorter; MMS, methylmethanesulfonate; HU, hydroxyurea.

⁴ M. Singh and B. D. Preston, unpublished data.

(including its native promoter) cloned into the *LEU2* plasmid YCplac111 (ATCC). Nineteen oligonucleotides and their complementary sequences, each pair encoding a different amino acid at position 612, were used in PCRs with YCplac111-*POL3* to generate the desired mutations. All of the primer sequences are available upon request. The presence of the predicted mutation at codon 612 and the absence of additional mutations were established by sequencing the entire *pol3* gene, which was then excised from the vector by digestion with HindIII/EcoRI and cloned into fresh YCplac111 vector digested with the same enzymes. The resulting haploid mutant strains were used for this work. Plasmid shuffling, modeled after the procedure of Simon *et al.* (29), was used to create Pol δ mutant strains. Plasmids harboring point mutations at Leu⁶¹² were transformed individually into YGL27-*pol3* Δ cells by using an EZ-transformation II kit (Zymo Research, Orange, CA). Transformed cells were grown on SC-Leu-Ura plates (28) for 2–3 days to select for both the YCplac111-*pol3*, (*pol3* mutants, *LEU2* marker) and pGL310 (*POL3*, wild type, *URA3* marker) plasmids. Controls included transformations with YCplac 111 (vector alone), wild type *POL3* and the exonuclease-deficient *pol3-01* allele (D321A,E323A) in YCplac111 (29). The pGL310-*POL3* plasmid was shuffled out by streaking 10–20 colonies on SC-Leu (28) plates containing 5-fluoroorotic acid (ZymoResearch, Orange, CA; 1 mg/ml). Colonies that grew were re-streaked on fresh SC-Leu + 5-fluoroorotic acid plates. After 2–3 days, *LEU2* plasmids were rescued from three independent colonies of each “shuffled-out strain” and sequenced to verify the predicted mutations. The same procedures were used to construct *pol3* mutant derivatives in a BY4741 strain background; the haploid BY4741-*pol3* strains were used for FACS analysis, because of their facile synchronization with α mating factor and the inability of YGL27-3D strains to respond to α mating factor.

Quantitation of *POL3* mRNA Expression—Two-step real time reverse transcription-PCR was used to quantitate *POL3* mRNA expression. Overnight cultures of each of the strain were diluted to $A_{600\text{ nm}} = \sim 0.2$, cultured at 30 °C, and harvested at $A_{600\text{ nm}} = \sim 0.7$. Total RNA was isolated using a hot phenol procedure, and 2 μg of RNA was digested with RQ1 DNase (Promega, Madison, WI) to hydrolyze contaminating genomic DNA. cDNA synthesis and PCR was performed using a SuperScript III Platinum Two-step qRT-PCR kit with SYBR Green (Invitrogen) according to the manufacturer’s instructions. Real time PCR was performed on a DNA Engine Opticon2 instrument and analyzed with the supplied software (Bio-Rad). *POL3* mRNA levels were quantitated and normalized to the constitutively generated *URA3* transcript. Standard curves for both *POL3* and *URA3* transcript were generated by plotting the threshold of signal detection against the log of RNA dilution. The amount of RNA used in each reaction was in the linear range as observed from the *POL3* and *URA3* standard curves. The threshold values $C(t)$ obtained from amplification profiles were first normalized to the internal standard *URA3* and next to the wild type *POL3* level. The entire procedure was repeated with changes in the RNA amounts used in cDNA synthesis. PCR primers and cycling conditions are available upon request.

Spontaneous Mutation Rate and Mutation Spectra—Fluctuation analysis was used to determine forward mutation rates at the *CAN1* (arginine permease) locus. The cells were grown overnight in SC-Leu medium (28), serially diluted, plated on SC complete medium (28), and incubated for a week or until the colonies reached 2–4 mm in diameter. Nine colonies from each strain were excised from the agar plates, suspended in sterile H₂O, and dispersed by vortexing and sonication. The aliquots were removed to count the total number of cells, and the remainder was plated on SC-Leu-Arg medium containing canavanine sulfate (Sigma; 60 mg/ml) to select for canavanine-resistant (Can^r) cells.

After 2–4 days, the number of Can^r colonies was counted, and the mutation rate was evaluated by using the method of the median of Lea and Coulson (30). Mutations in independent Can^r colonies were verified by PCR amplification of ~ 1.8 kb of *CAN1* genomic DNA using high fidelity Ultra *Pfu* DNA polymerase (Stratagene, CA), followed by purification and direct sequencing of the amplified DNA. Sequences of primers used for PCR and DNA sequencing are available upon request.

Flow Cytometry Analysis—Fresh saturated overnight cultures were diluted to $A_{600} = \sim 0.3$ –0.4, cultured at 30 °C for 1 h, and synchronized by the addition of 10 $\mu\text{g}/\text{ml}$ of α mating factor; after 2.5 h, the cells were microscopically examined for synchrony, washed twice in sterile distilled water, and dispersed in prewarmed YPD. 1 ml of cells was removed every 30 min for 300 min, and the cells were spun down and fixed in 100% ethanol. The fixed cells were washed once in 10 mM Tris-HCl (pH 7.5), 10 mM EDTA suspended in 0.1 ml of 10 mM Tris-HCl (pH 7.5), 10 mM EDTA, 0.1 mg/ml RNase A and incubated overnight at 37 °C. The cells were digested with proteinase K at a final concentration of 0.1 mg/ml by incubation at 55 °C for 50 min. Thereafter the cells were pelleted, washed once in 1 \times phosphate-buffered saline, 1 mM EDTA, and suspended in 0.1 ml of 1 \times phosphate-buffered saline, 1 mM EDTA, 100 $\mu\text{g}/\text{ml}$ propidium iodide. The stained cells were diluted 10 times in 1 \times phosphate-buffered saline, 1 mM EDTA, sonicated, and sorted on a BD Biosciences flow cytometer.

RESULTS

Eight Replacements for *S. cerevisiae* Pol δ Leu⁶¹² Yielded Viable Mutants—To assess the function of Leu⁶¹² in motif A of *S. cerevisiae* Pol δ , we used site-directed mutagenesis to create all 19 amino acid replacements. Sequence and structural conservation of motif A residues in family A and family B DNA polymerases of particular interest for this work are illustrated in Fig. 1 (A and B). A model of the active site of RB69 DNA polymerase, a family B member, that shows Leu⁴¹⁵, the residue homologous to Leu⁶¹² in yeast Pol δ , is illustrated in Fig. 1C.

Of the 19 replacements for Leu⁶¹² in yeast Pol δ , we found that eight yielded viable haploid mutant strains: Ile, Val, Thr, Phe, Met, Lys, Asn, and Gly. The mutant strains formed colonies at 25, 30, and 37 °C on both rich (YPD) and minimal (SC-Leu) media; however, for L612G and L612N, colony formation and mid-log phase growth in rich and minimal media were slower when compared with wild type and other mutant strains. All of the other strains exhibited a doubling time at mid-log phase similar to that of wild type cells in YPD medium at 30 °C (data not shown).

Leu⁶¹² Mutants Displayed Differential Hypersensitivity to Hydroxyurea and MMS—The essentiality of Pol δ for DNA replication implies that substitutions for Leu⁶¹² might confer hypersensitivity to genotoxic agents. We therefore grew the mutants on YPD containing hydroxyurea (HU), an inhibitor of ribonucleotide reductase that diminishes dNTP pools and thereby causes replication forks to stall (31). For reference, we included the exonuclease-minus, proofreading-deficient mutant *pol3-01* (D321A,E323A) (29, 32). As shown in Fig. 2, most of the Leu⁶¹² mutants exhibited reduced growth relative to that of the wild type strain on YPD containing 50 mM HU. The variation in sensitivity was wide, with L612M being minimally affected, if at all, and L612T, L612G, and L612N being severely inhibited. The relative sensitivity was as follows: Leu⁶¹², *pol3-01*, L612M < L612I, L612V, L612F < L612K, L612G, L612T, L612N. The greater inhibition of L612I relative to L612M was clearly evident at 75 mM HU, where L612I was inviable, and both L612M and *pol3-01* grew weakly (data not shown). We conclude that the majority of the viable Leu⁶¹² mutants are hypersensitive to HU and infer that

Yeast Pol δ Leu⁶¹² Substitutions Induce Mutator Phenotypes

FIGURE 1. Motif A structure in family A and family B DNA polymerases and modeled active site. A, amino acid sequence alignment of motif A residues. Leu⁶¹² in *S. cerevisiae* Pol δ , which was analyzed here, and its homologs, are boxed. B, structural alignment of motifs A, B, and C in family A and family B DNA polymerases, illustrating strict conservation. The α backbone is shown. The star highlights the conserved aliphatic residue corresponding to Leu⁶¹² in *S. cerevisiae* Pol δ . Coordinates of crystal structures were obtained from Protein Data Bank (www.rcsb.org) and manipulated in SwissPDB viewer v3.5 software (www.expasy.ch). Motifs A, B, and C of the polymerase active sites were superimposed, and root mean square deviations were calculated using the tools available in the software. The family A polymerases shown are: the Klenow fragments of DNA polymerase I from *E. coli* (Protein data base code 1KFD, black) and *Thermus aquaticus* (KlenTaq, Protein data base code 3KTQ, blue); T7 (bacteriophage T7, Protein data base code 1T7P, green); and Bst (*Bacillus stearothermophilus*, Protein data base code 1XWL, brown). The family B DNA polymerases shown are: RB69 (bacteriophage RB69, Protein data base code 1IG9, red); Tgo (*Thermococcus gorgonarius*, Protein data base code 1TGO, purple); D.Tok (*Desulfurococcus tok*, Protein data base code 1QQC, yellow); and KOD (*Pyrococcus kodakaraensis*, Protein data base code 1GCX, cyan), root mean square deviation ranges from 0.5 to 1.5 Å. C, polymerase active site in a ternary complex (Protein data base code 1IG9) of the family B RB69 DNA polymerase with an oligonucleotide primer-template and dTTP (54, 55). Leu⁴¹⁵ (the homolog of Leu⁶¹² in *S. cerevisiae* Pol δ) is shown in ball-and-stick form, and is in close proximity to the sugar and α -phosphate of the incoming dTTP. The figure is labeled as follows: green A, motif A; tan B, motif B; blue C, motif C; silver-gray P, primer strand; blue-gray T, template strand. Dark gray balls depict divalent calcium ions.

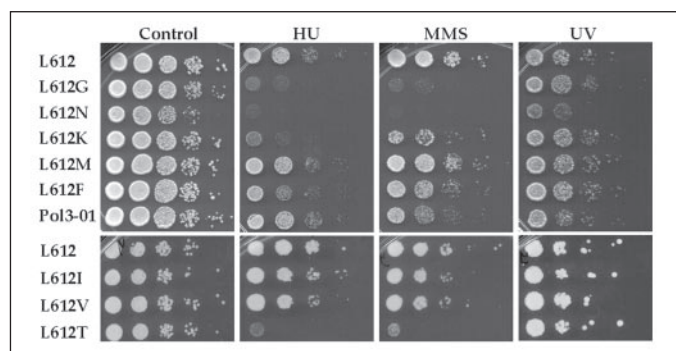
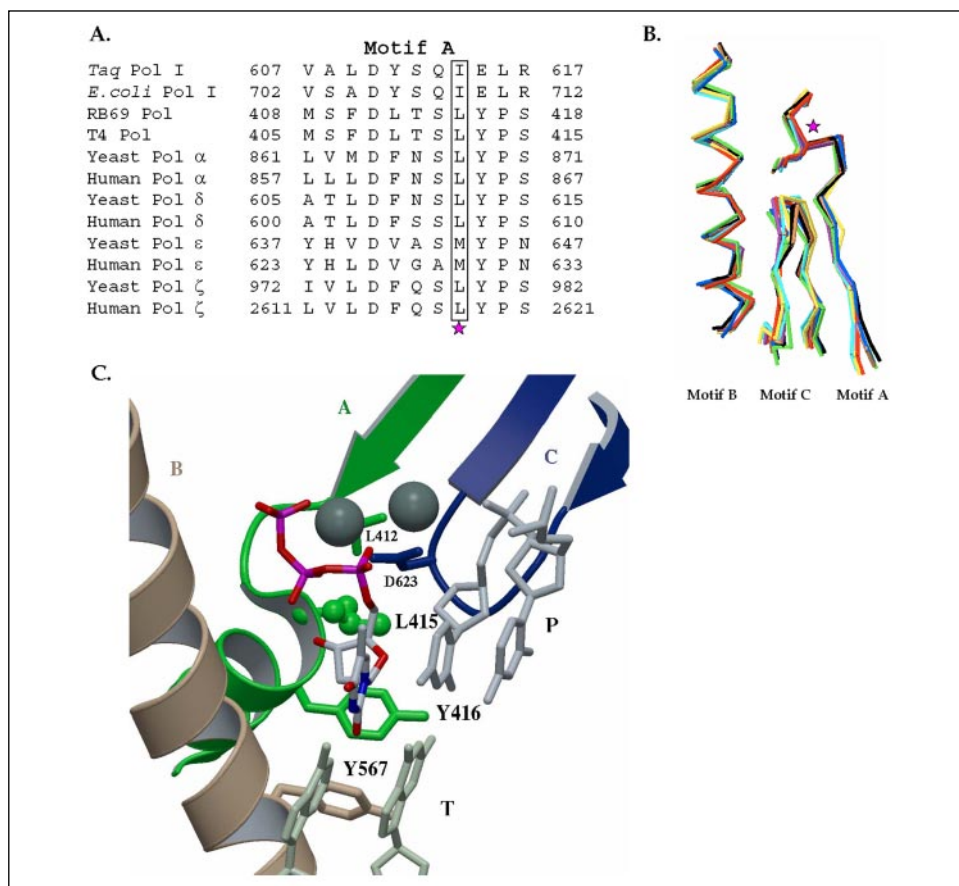


FIGURE 2. Sensitivity of Leu⁶¹² mutants to genotoxic agents. Overnight cultures of YGL27-derived haploid strains were dispersed by sonication, and cell number was counted. The cells were serially diluted 10-fold in a 96-well microtiter plate, starting with 1×10^7 cells/ml, and spotted on YPD plates by using a 48-prong (prong replicator capable of transferring 48 samples) replicator. Incubation was at 30 °C for 2–3 days. The plates contained either no additions (control), 0.025% MMS, or 50 mM HU; UV-irradiated plates (100 J/m^2) were incubated in the dark.

Leu⁶¹² in wild type Pol δ supports the ability to carry out DNA synthetic processes in the presence of reduced dNTP concentrations.

To assess the effects of replacement of Leu⁶¹² on sensitivity to alkylation, we exposed the mutants to the methylating agent MMS. MMS introduces diverse methyl adducts in DNA and also causes replication forks to stall (33, 34). Most of the eight Leu⁶¹² mutants showed reduced viability relative to the wild type strain when grown on YPD containing 0.025% MMS (Fig. 2). The relative hypersensitivity of the mutants was similar to that observed for HU: L612, L612M, L612I, L612V < L612F, *pol3-01* < L612K < L612G, L612T, L612N. As in the case of HU, MMS hypersensitivity varied greatly, from slight if any (L612M, L612I, and L612V) to severe (L612G, L612T, and L612N). The reduced MMS

resistance in many of the mutants may be indicative of a deficit in one or more of the processes in which *S. cerevisiae* Pol δ participates, e.g. replication, base excision repair of methylation damage, and/or recombination (4, 35, 36).

In contrast to the results for MMS, the Leu⁶¹² mutants showed wild type growth following UV irradiation at doses up to 100 J/m^2 , with the exception of L612N (Fig. 2). Other Pol δ mutants as well do not display hypersensitivity to UV, a finding that has been ascribed to the function of other DNA polymerases, such as Pol ϵ or Pol η , in repair or tolerance of UV damage (35, 37, 38). However, the exceptional L612N mutant may be so severely impaired that redundant functions cannot fully compensate, thus unmasking a contribution of Pol δ to UV survival.

Leu⁶¹² Mutant Strains Exhibited Varying Cell Cycle Defects and Morphologic Anomalies—Based on the role of Pol δ in replication and the HU and MMS hypersensitivity described above, we looked for evidence of anomalous cell cycle progression in the Leu⁶¹² mutants. As shown in the FACS analyses in Fig. 3, substitutions at Leu⁶¹² produced cell cycle defects of differing kinds and degree. Also, as summarized in Fig. 4A, mid-log cultures of some mutant strains contained cells with aberrant morphology. Representative morphologic anomalies in the mutant cultures, together with representative wild type cells, ascertained by phase contrast microscopy and nuclear staining of at least 600 cells for each strain, are depicted in Fig. 4B. We describe the less affected mutants first and proceed to the most anomalous. The L612I, L612V, L612G, and *pol3-01* mutants appeared to initiate DNA synthesis somewhat more slowly than the wild type strain after release from α -factor arrest, as judged by an excess of cells with 1 n DNA content at 30 min (Fig. 3). A similar delay has been observed previously for another *pol3-01* strain (39). In addition, the L612V mutant accumulated a disproportionately

large fraction of cells with DNA content intermediate between 1 and 2 N at 30 and 90 min, suggestive of prolonged S phase. The L612T strain also showed this latter pattern. The L612M strain exhibited minimal deviation

from wild type profiles, apart from a possible excess of cells with a DNA content intermediate between 1 and 2 N at 30 min, suggestive of slow S phase progression. The L612K strain also displayed minimal deviation in FACS analysis, although the unsynchronized culture contained an elevated fraction of cells with 2 N DNA content, and an apparently elevated proportion of cells with 2 N DNA content was not synchronized in G₁ by α-factor.

The L612G mutant was conspicuously anomalous. We observed an excess of cells with 1 N DNA content, as well as a DNA content intermediate between 1 and 2 N, through the initial 90 min after release from arrest. We infer that there is a delay in the onset of DNA synthesis in the L612G mutant and slow traverse of the first S phase following arrest. By 120 min after release, the profile in the L612G mutant resembled that in the wild type strain at 90 min, most of the cells in both cultures having reached 2 N DNA content. After 120 min, progression in the L612G mutant paralleled that seen in the wild type strain after 90 min. Morphologic analysis of a mid-logarithmic phase culture (Fig. 4) showed a high proportion of aberrant cells, including an approximately 4-fold excess of large budded dumbbell-shaped cells with divided or undivided nuclei at or near the bud neck, suggestive of G₂/M arrest.

The L612N mutant showed the most severe cell cycle defects. An unsynchronized culture, as well as cultures examined at ≥90 min after release from arrest, accumulated a large population of cells with 2N DNA content, suggestive of G₂/M arrest (compare 2 N peak at 90 min with 210 min in Fig. 3). Consistent with this inference, an 8-fold excess of cells in a mid-log phase culture (40% versus 5% for wild type) were dumbbell-shaped with undivided nuclei at or near the bud neck (Fig. 4). Additionally, the 30-min FACS profile was suggestive of prolonged S phase (Fig. 3).

The apparent prolongation of S phase and/or presence of a large fraction of cells with G₂/M arrest phenotype in some of the mutants is suggestive of activation of DNA damage-induced checkpoint arrest. To support this interpretation, we confirmed that the *Leu*⁶¹² mutants are proficient in checkpoint activation. To establish this proficiency, we used a sensitive checkpoint activation reporter in which the promoter of the damage-inducible *RNR3* gene is fused to the *E. coli lacZ* gene encoding β-galactosidase (40). As shown in Fig. 5, the mutants expressed

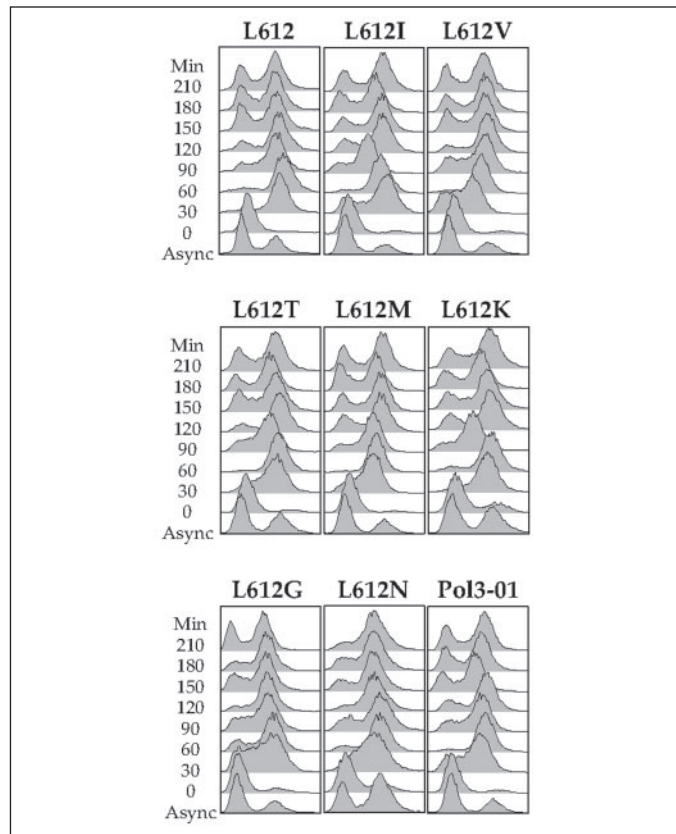


FIGURE 3. Cell cycle progression of *Leu*⁶¹² mutants. Cultures of BY4741-derived haploid strains at $A_{600\text{ nm}} \sim 1.8\text{--}2.6$ were freshly diluted to $A_{600\text{ nm}} \sim 0.3\text{--}0.4$ in YPD and synchronized by the addition of 10 μg/ml of α mating factor. After 2.5 h, the cells were examined microscopically for synchrony, pelleted, washed twice with sterile distilled water, and incubated in prewarmed YPD. The aliquots were removed at 30-min intervals, and cells were spun down and fixed in 100% ethanol. Fixed cells were processed as mentioned under “Experimental Procedures” and sorted by utilizing a BD Biosciences fluorescence-activated flow cytometer, and the cell cycle profiles were analyzed using the program Flowjo (Ashland, OR).

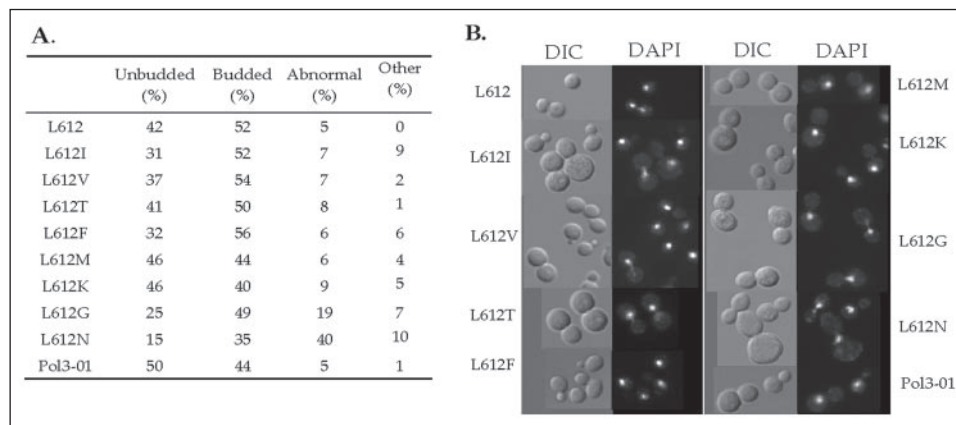


FIGURE 4. Cellular and nuclear morphology of *Leu*⁶¹² mutants. Aliquots of mid-logarithmic phase cultures of YGL27-derived haploid strains ($A_{600} \sim 0.7\text{--}1.2$) were used to examine cellular morphology by phase contrast (differential interference contrast) microscopy. For nuclear morphology, cells were fixed in 70% ethanol and stained with Vectashield mounting medium (Vector Laboratory) containing 4',6'-diamidino-2-phenylindole (DAPI). The images were acquired at 63× magnification using a Qimaging Retiga EX digital camera mounted on a Nikon Eclipse E600 microscope. At least 600 cells of each mutant strain were examined in each of two independent experiments. A, the proportions of cells observed in mutant strains are indicated, ascertained by examination of no fewer than 600 cells/strain in each of two independent experiments. The average of both experiments is tabulated. Unbudded cells are in the G₁ phase. Budded cells are in the S phase or the normal G₂/M phase. Abnormal cells are large budded, dumbbell-shaped cells with an undivided or divided nucleus, indicative of G₂/M phase (predominant fraction) and post-M phase arrest, respectively. Other cells are comprised of abnormally large budded, unequal sized mother-daughter cells, multiple-budded cells, and elongated cells. B, differential interference microscopy (DIC) images of representative anomalous cells in mutant cultures and images of the same DAPI-stained cells are shown.

Yeast Pol δ Leu⁶¹² Substitutions Induce Mutator Phenotypes

β -galactosidase when challenged with MMS, at essentially the same level as the wild type strain.

Substitutions for Leu⁶¹² Generated a Mutator Phenotype—Replacement of residues homologous to Leu⁶¹² in motif A in DNA polymerases from families A, B, and Y can alter fidelity (12, 14, 15, 20–22, 41, 42). Depending upon the polymerase and allele, either an increase or decrease in mutation rate and/or altered mutation frequency *in vitro* and/or *in vivo* have been observed. To ascertain whether replacement of Leu⁶¹² in our yeast Pol δ mutants generates mutator and/or anti-mutator phenotypes, we measured forward mutation rates at the *CAN1* (arginine permease) locus in the eight viable strains. As summarized in Table 1, we observed a continuum of mutation rates from near wild type (L612I, L612V, and L612T) to 37-fold elevated (L612N). The largest elevations were obtained for L612K (13-fold), L612G (17-fold), and L612N (37-fold), the increase for L612N being similar to that seen for the *pol3-01* mutant lacking exonucleolytic proofreading (29-fold) (29, 32, 43). The increase for L612M (7-fold) is in accord with the 3.5-fold elevation recently reported (44). Interestingly, the increase in mutation rate was not strictly correlated with other phenotypic deficiencies. For example, the L612M mutant exhibited an increased mutation rate together with slight, if any, sensitivity to HU and MMS. Conversely, the L612T mutant showed little if any elevation of mutation rate together with marked hypersensitivity to HU and MMS. To ensure that the Leu⁶¹² substitution strains were not exhibiting mutator phenotypes

because of altered expression of Pol δ , we quantitated the mRNA levels of Pol δ in all of our strains and normalized them to wild type strain. Pol δ mRNA levels were determined by quantitative reverse transcription-PCR using purified total RNA obtained from each of the strains during exponential growth. The fold change in RNA levels in the strains that displayed the most profound phenotypic defects, L612K (13-fold), L612G (17-fold), and L612N (37-fold), was increased 2.5-, 1.5-, and 2.8-fold, respectively. In contrast, the level in the reference exonuclease deficient strain, *pol3-01*, was reduced 1.7-fold compared with that of the wild type. Furthermore, the expression levels in strains that did not significantly affect mutation rates, L612I, L612V, L612F, and L612M, were +1.1, –3.5, –1.3, and –1.6-fold compared with that of the wild type, respectively. Our analysis suggests that each different substitution for Leu⁶¹² elicits unique phenotypic defects, and these defects do not correlate with small changes in the Pol δ mRNA expression levels or changes in mutation rates.

To examine the nature of the mutations arising in the Leu⁶¹² variants, we sequenced the 1.8-kb *CAN1* gene in independent canavanine-resistant (Can^r) clones. As summarized in Table 2 and consistent with previous reports (37, 39, 45), the most frequent mutations in the wild type strain were single-base substitutions, with transitions outnumbering transversions. The remaining mutations were insertions or deletions. A notable feature of the wild type spectrum was the presence of mononucleotide runs of at least three As or Ts immediately 5' or 3' of the mutation in 52% (12 of 23) of the Can^r clones. An apparent propensity of wild type strains for mutations at mononucleotide runs has been observed by others (37, 39, 45). The mutation spectra observed for the five Leu⁶¹² mutant strains with the highest mutation rates did not differ substantially from the wild type spectrum (Fisher's exact test) base substitutions representing the majority of sequence changes. The L612K spectrum, however, is statistically distinct (Fisher's exact test, $p = 0.01$) from the rest in including more transversions than transitions; in fact, 28% of all mutations (5 of 18) were T \rightarrow A transversions (46). The L612K spectrum also contained the largest proportion of insertions/deletions.

DISCUSSION

In this work, we used site-specific mutagenesis and plasmid shuffling to create all 19 replacements for the highly conserved Leu⁶¹² in motif A of *S. cerevisiae* Pol δ (Fig. 1). Our rationale was based on the essential roles of Pol δ in DNA synthetic processes in eukaryotic cells and on the importance of residues homologous to Leu⁶¹² for replication fidelity of other DNA polymerases. Eight of the 19 replacements for Leu⁶¹² supported growth, including the conservative substitutions Ile, Val, and Met, as well as the nonpolar aromatic Phe. These hydrophobic residues occur naturally at the homologous position in other DNA polymerases (Fig. 1) and/or are tolerated as single substitutions in *E. coli* Pol I, *Taq*

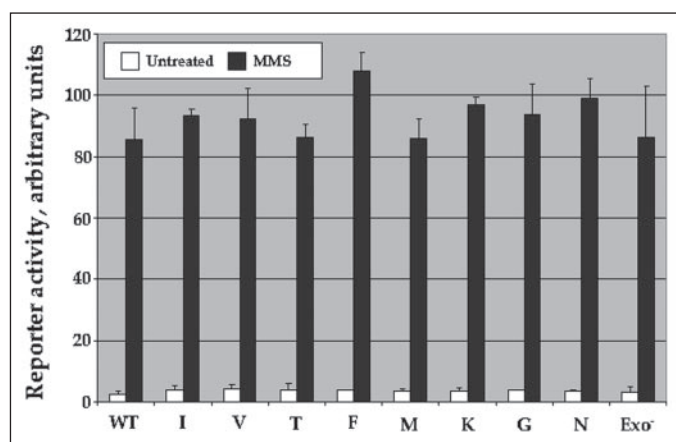


FIGURE 5. Activation of the DNA damage-inducible checkpoint reporter RNR3. The ability of the Leu⁶¹² mutants to activate a DNA damage-inducible checkpoint leading to G₂/M arrest was determined by using the reporter plasmid pZZ13. The plasmid, containing the promoter of the damage-inducible *RNR3* gene fused to *E. coli lacZ* (*RNR3-LacZ*) was transformed into YGL27-derived mutant cells. Cultures of all strains were diluted to A₆₀₀ = 0.2–0.25, incubated at 30 °C with and without 0.012% MMS for 5 h. Triplicate samples of MMS-treated and untreated control cells were assayed for β -galactosidase activity by monitoring hydrolysis of *o*-nitrophenyl- β -galactopyranoside (40).

TABLE 1

Forward mutation rates at *CAN1* in strains with an amino acid substitution at Leu⁶¹² in conserved motif A of DNA polymerase δ

Spontaneous mutation rates were measured by fluctuation analysis using the method of the median as described under 'Experimental Procedures.' Two independent experiments were performed. Fold elevation indicates the average of the two experiments listed relative to the average for the wild type Leu⁶¹². The *pol3-01* strain contains the exonuclease proofreading-deficient Pol δ allele D321A,E323A (32).

Strain	Rate/cell division ($\times 10^{-7}$)			Fold elevation
	Experiment 1	Experiment 2	Mean (95% CI)	
Leu ⁶¹²	1.5	2.4	2.0 (1–3)	1
L612I	2.0	4.7	3.4 (1–6)	2
L612V	2.7	3.3	3.0 (2–4)	2
L612T	3.6	3.7	3.7 (3–4)	2
L612F	5.6	8.4	7.0 (4–10)	4
L612M	11	18	15 (8–21)	7
L612K	19	32	26 (13–38)	13
L612G	45	20	33 (8–57)	17
L612N	46	100	73 (20–126)	37
<i>pol3-01</i>	50	62	56 (44–68)	29

TABLE 2

Mutational spectra at the *CAN1* locus in DNA polymerase δ Leu⁶¹² mutant strainsThe mutational spectra were determined by DNA sequencing of PCR-amplified *CAN1* genomic DNA from independent Can^r clones.

Errors	Leu ⁶¹²	L612F	L612M	L612K	L612N	L612G
Total	23 ^a	20	21 ^b	18	27 (14)	20 ^c
Base substitutions	17 (74%)	14 (70%)	18 (86%)	13 (65%)	25 (93%)	19 (95%)
Transitions						
A → G				1	1	
C → T				1	14 (1) ^d	
G → A	6	2	11		2	12
T → C	5	7	5	3		1
Total	11	9	16	5	17 (4)	13
Transversions						
A → C				1		
A → T	2				1	1
C → A	1	3	2		1	2
C → G	1			1		
G → C	1			1	1	
G → T		1				2
T → A		1		5	5	1
T → G	1					
Total	6	5	2	8	8 (8)	6
Deletions	4 (17%)	6 (30%)	1 (5%)	7 (35%)	2 (7%)	1 (5%)
Insertions	2 (9%)	0	2 (10%)	0	0 (0)	0

^a Two Can^r wild type clones had two independent mutations.^b Two Can^r L612 M clones had two independent mutations.^c One Can^r L612G clone had two independent mutations.^d 14 independent Can^r clones carried an identical mutation, perhaps because of a jackpot event.

Pol I, and/or yeast Pol α (12, 14, 15, 20, 41). The nonconservative substitutions Thr and Lys, and to a lesser extent Asn, have also been found among single replacements tolerated in Pol I, whereas Gly has not been observed (12, 14, 15, 20, 41).

Allele Dependence of Phenotype among Leu⁶¹² Mutants—We examined the sensitivity of the viable mutant strains to genotoxic substances, cell cycle progression and cellular morphology, and forward mutation rate and spectra at the *CAN1* locus. Our data suggest that none of the viable mutant alleles is phenotypically silent, highlighting the importance of Leu⁶¹² for Pol δ function. Given their location at the polymerase active site (Fig. 1), the mutant amino acids may affect catalytic efficiency, base selection fidelity, processivity, and other crucial properties of the mutant polymerases. We observed a wide range in the severity of phenotypic defects, the more conservative replacements being less deleterious overall. However, there was not a strict association of specific defects among the individual mutants; this allele-dependent dissection of phenotypic deficits suggests that the mechanism(s) underlying any particular defect may differ among the mutants. We observed small fluctuations in the total mRNA levels and found no direct correlation between mRNA expression and phenotypic defects among the strains. For example, the strains L612K, L612G, and L612N that displayed elevated mutation rates and other phenotypic defects expressed a 2–3-fold higher mRNA level compared with the wild type, whereas the reference strain *pol3-01*, which also exhibited a high mutation rate, displayed a 2-fold lower level compared with the wild type. A similar variation was observed in strains that exhibited only minimal alterations in mutation rates.

Each viable replacement for Leu⁶¹² appeared to yield a unique combination of functional deficits. The Ile, Val, and Thr substitutions had little, if any, effect on the mutation rate (Table 1). Ile and Val were relatively innocuous overall, although both mutants showed a delay entering S phase after release from α -factor arrest (Fig. 3), and a particularly large fraction of L612I cells had aberrant morphology for reasons that are not apparent (Fig. 4). In contrast, Thr conferred marked hypersensitivity to HU and MMS (Fig. 2), together with slow S phase traverse in the first and second cycles after α factor arrest, possibly indicative of a defect in replication and/or repair of methylation damage. The Phe

substitution conferred intermediate levels of deficiency overall, including a 4-fold elevation of mutation rate (Table 1), and we observed predominantly base substitution errors.

The L612M replacement is of particular interest, conferring a 7-fold elevation of mutation rate (Table 1), with minimal effect on the other properties examined. Apparently, the modestly error-prone L612M polymerase supports nearly normal replication. This is the case even when cells are grown in the presence of HU, which requires DNA synthesis at low dNTP concentrations, or MMS, which requires concurrent Pol δ -mediated replication and base excision repair (35). Based on the relative replication proficiency and the predominance of base substitutions in the mutation spectrum (86%; Table 2), we hypothesized that the L612M mutator phenotype may reflect mainly errors made by the polymerase, rather than secondary mutagenic processes induced by defective replication. The recent work of Li *et al.* (44), which was published as we completed this manuscript, sheds light on the function of the L612M polymerase. These authors also observed a mutator phenotype; the rate of forward mutation at *CAN1* was elevated 3.5-fold, consistent with our results. Li *et al.* further ascertained that mutation rates were increased in the absence of core mismatch repair proteins. The dependence of mutation rate on mismatch repair, which corrects errors that escape proofreading, suggests that the L612M mutator phenotype may in fact reflect errors made by the mutant polymerase. The L612M mutant also exhibited evidence of compromised replication, namely inviability in the absence of the *RAD27* flap endonuclease that processes Okazaki fragments, and hypersensitivity to phosphonoacetic acid, a replication inhibitor that may act as a pyrophosphate analog. Therefore, it is also possible that replication defects in the L612M mutant may induce secondary mutagenic processes that contribute to the observed mutator phenotype.

The Leu⁶¹² Lys, Gly and Asn replacements produced the most defective mutants overall, conferring the highest mutation rates (Table 1) together with markedly reduced growth in the presence of HU and MMS (Fig. 2). Growth of the L612N mutant was impaired even in the absence of exogenous agents (*e.g.* Fig. 2 and data not shown). Each of the three mutants showed anomalies in cell cycle distribution and/or morphology that are indicative of slow S phase progression and/or arrest at

Yeast Pol δ Leu⁶¹² Substitutions Induce Mutator Phenotypes

G_2/M phase (Figs. 3 and 4). For example, asynchronous cultures of the L612K contained an excess of cells with 2 N DNA content, indicative of G_2/M arrest. The L612G mutant was delayed entering the S phase following release from α -factor arrest, was slow to traverse S phase in the first cycle and accumulated an increased proportion of large budded, dumbbell-shaped cells that are characteristic of G_2/M arrest. The L612N mutant exhibited a slow S phase and multiple, pronounced defects predominantly indicative of G_2/M arrest, including an 8-fold excess of large budded, dumbbell-shaped cells. Detection of G_2/M arrested cells (Fig. 4) presumably reflects activation of a DNA damage-induced checkpoint pathway(s) triggered by endogenous DNA damage (47, 48). This damage could be polymerase errors *per se*, e.g. mispaired primer termini that are not efficiently proofread and lead to frequent replication fork stalling (49). The inviability of the L612K, L612G, and L612N mutants in combination with the exonuclease-minus *pol3-01* allele (data not shown) supports this interpretation. Alternatively, or in addition, the damage could be defects in newly synthesized DNA arising from reduced catalytic efficiency or altered processivity, perhaps resulting in uncoupling of lagging strand from leading strand synthesis. Whatever the nature of the damage, the poor viability in HU and MMS, and accumulation of cells with G_2/M checkpoint arrested morphology suggests perturbations at replication forks.

In budding yeast, replication forks play a critical role as both activators and primary effectors of an S phase checkpoint pathway(s), and the activated checkpoint pathway(s) in turn leads to stabilization of stalled forks by retarding new DNA synthesis and arresting cells at G_2/M phase (33, 50, 51). Finally, the mutation spectra we observed for the Lys, Gly, and Asn replacements further highlights the allele dependence of phenotypes conferred by Leu⁶¹² substitutions. Although all three spectra were dominated by base substitution errors, the L612K spectrum contained a notably high proportion of transversions and the largest fraction of deletion events observed. Interestingly, we have observed that PCR-generated mutant libraries created utilizing the *Taq* Pol I mutant I614K (homologous to the yeast L612K mutant) contained ~20% of clones with deletion events, whereas wild type *Taq* Pol I produced no deletion events (data not shown). Therefore the nonconservative substitutions at the Leu⁶¹² position in Pol δ confer strong cell cycle phenotypes during S phase progression and lead to G_2/M phase arrest.

We utilized the *pol3-01* mutant throughout this work to compare the effects of proofreading exonuclease deficiency with the effects of replacement at Leu⁶¹² in the polymerase active site. The mutation rate of the *pol3-01* mutant was elevated ~30-fold (Table 1), and the mutation spectrum suggests that *pol3-01* cells accumulate base substitution errors, consistent with previous observations (32, 39, 43). Despite the increased mutation rate, the *pol3-01* mutant exhibited a nearly normal phenotype in other respects. HU and UV sensitivity were like wild type, and MMS sensitivity was moderately increased (Fig. 2). As previously observed, the *pol3-01* cells exhibited only subtle cell cycle defects, *i.e.* a slight delay in entry into the S phase after release from α factor arrest (39), similar to that seen for L612I, L612V, L612T, L612M, L612G, and L612N cells. A further increase in abnormal cellular morphologies was not observed at mid-logarithmic phase. Taking the *pol3-01* phenotype as a reference, we conclude that an elevated mutation rate *per se* is not sufficient to account for the broad range of phenotypes observed among the Leu⁶¹² alleles. We propose that replacement of Leu⁶¹² may result in additional replication defects and concomitant DNA damage that causes perturbation at replication forks.

The Mutator Phenotype in Leu⁶¹² Mutants—Replication fidelity is altered by replacement of residues homologous to Leu⁶¹² in several other DNA polymerases. Our laboratory has previously found that spe-

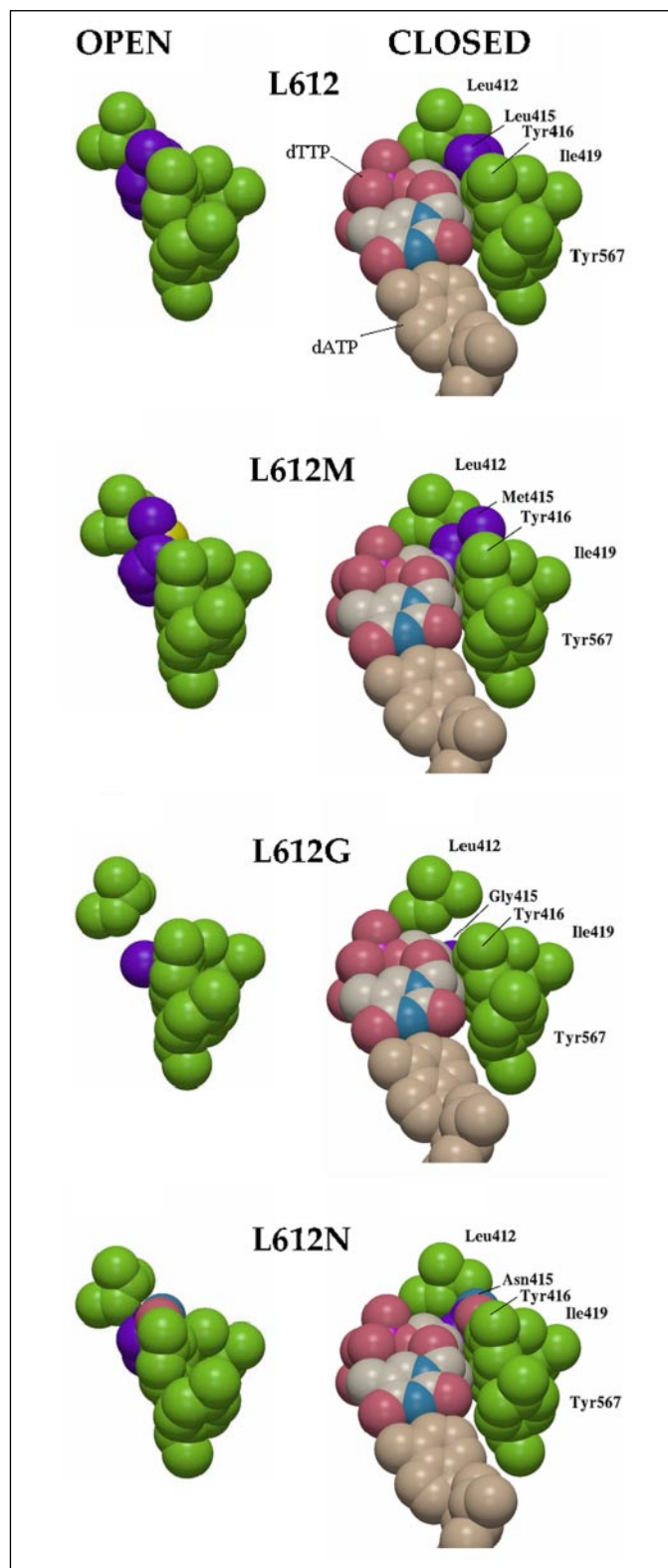


FIGURE 6. Molecular models of RB69 DNA polymerase mutants homologous to *Saccharomyces cerevisiae* Pol δ Leu⁶¹² mutants. Coordinates of the open and closed structures of the family B RB69 gp43 DNA polymerase were obtained from the Protein Data Bank (codes 1IH7 and 1IG9, respectively). Mutations at Leu⁴¹⁵, the residue homologous to yeast Pol δ Leu⁶¹² (Fig. 1, A and B) were modeled with tools available in the suite of programs in the Molecular Operating Environment (www.chemcomp.com). Coordinates for residues within 12 Å of the mutated residue, including the nucleotides, were energy-minimized using Engh and Huber structural parameters and standard procedures available in the Molecular Operating Environment package. The figures were generated using MOLSCRIPT and Raster3Dv2.0.

cific substitutions for the homologous Ile residue in *E. coli* Pol I and *Taq* Pol I, members of the A family of DNA polymerases, yield mutator mutants (12, 15). For example, the I709F mutant of *E. coli* Pol I increases mutation frequency *in vitro* and *in vivo* while maintaining wild type catalytic efficiency (12). Among family B DNA polymerases, the L415M substitution in phage T4 DNA polymerase creates a mutator mutant that exhibits wild type polymerase activity, increased processivity, and reduced exonuclease activity; available evidence indicates that the L415M polymerase cannot efficiently initiate transfer of DNA from the polymerase active site to the exonuclease active site, effectively reducing proofreading. The L415I substitution in T4 DNA polymerase generates an anti-mutator (21), whereas the L612I mutant of yeast Pol δ appears to have near wild type fidelity (Table 1). In this case, the effects of a specific replacement differ widely, indicative of interactions of the Ile substitution with other, polymerase-specific determinants of fidelity. In *S. cerevisiae* Pol α , the Phe, Met, Trp, and Val substitutions for the homologous Leu⁸⁶⁸ create mutators of varying strength, and the human L865F polymerase is also a mutator (20). In the more distantly related family Y translesion DNA polymerases, replacement of the homologous Phe³⁴ with Leu affects the accuracy of DNA synthesis as well (20). This brief survey indicates that wild type Leu⁶¹² in yeast Pol δ shares an important function in fidelity with homologous residues over a broad evolutionary spectrum. The Pol δ mutants with differing mutagenic potential that we have created will be of particular value for ascertaining the mechanisms by which Leu⁶¹² contributes to wild type replication and repair in a genetically facile eukaryotic model system.

Wild type DNA polymerase fidelity is conferred by active site geometry that accommodates a complementary Watson-Crick base pair but excludes incorrect pairs (52, 53). Proofreading of misincorporated nucleotides at the exonuclease active site contributes further to fidelity, and transit of the newly formed primer terminus between the polymerase and exonuclease domains is a crucial process affecting accuracy. The increased mutation rate caused by replacement of Leu⁶¹² in yeast Pol δ could reflect reduced discrimination against incorrect nucleotides at the polymerase active site. To assess this possibility, we modeled the amino acid substitutions into the active site of the family B RB69 DNA polymerase, in which Leu⁴¹⁵ is homologous to yeast Pol δ Leu⁶¹² (54, 55). The wild type RB69 polymerase and the L415M, L415G, and L415N mutant polymerases are illustrated in Fig. 6. Both the open conformation and a closed, ternary complex with an oligonucleotide primer template and incoming dNTP are shown for each. In the wild type ternary complex, the side chain of Leu⁴¹⁵ is in close proximity to the sugar and α -phosphate of the incoming dNTP and forms part of a hydrophobic region that includes Leu⁴¹², Tyr⁴¹⁶, and Tyr⁵⁶⁷. With the exception of the L415G polymerase, close study of the models revealed no obvious changes in active site geometry that might account for reduced fidelity. (The caveat, of course, is that available crystal structures may not capture conformations in which the mutations would be predicted to alter nucleotide discrimination.) In the case of the L415G polymerase, the absence of a side chain creates increased space and perhaps greater flexibility that might allow enhanced accommodation of incorrect nucleotides. We favor a model whereby the mutator phenotypes we observed may reflect, at least in part, inability of the Leu⁶¹² replacements to mediate proper partitioning between the polymerase and exonuclease active sites. This mechanism appears to contribute to the increased mutation rate of the T4 L415M polymerase (21).

In summary, we have created and analyzed a series of yeast Pol δ mutants by substitution of different amino acids for Leu⁶¹². Yeast expressing the mutant alleles exhibit diverse phenotypes that may differentially reflect the roles of Pol δ in various DNA synthetic processes.

An analysis of DNA synthesized *in vivo* by the mutant polymerases may help to delineate the roles of Pol δ in leading and lagging strand replication and in different DNA repair pathways. In addition, generation of mice harboring the mutant alleles should yield further information on the role of a mutator phenotype in the generation of tumors (56, 57).

Acknowledgments—We are grateful to Ellie Adman for molecular modeling and energy minimization calculations, for the drawings in Figs. 1C and 6, and for valuable discussions concerning structure-function relationships. We thank Mallika Singh for generating pol3::KanMX strains, Trisha Davis and Tess Yoder for technical help with flow cytometry, and Ann Blank for editing the manuscript.

REFERENCES

- Steitz, T. A. (1998) *Nature* **391**, 231–232
- Burgers, P. M., Koonin, E. V., Bruford, E., Blanco, L., Burtis, K. C., Christman, M. F., Copeland, W. C., Friedberg, E. C., Hanaoka, F., Hinkle, D. C., Lawrence, C. W., Nakanishi, M., Ohmori, H., Prakash, L., Prakash, S., Reynaud, C. A., Sugino, A., Todo, T., Wang, Z., Weill, J. C., and Woodgate, R. (2001) *J. Biol. Chem.* **276**, 43487–43490
- Hubscher, U., Maga, G., and Spadari, S. (2002) *Annu. Rev. Biochem.* **71**, 133–163
- Bell, S. P., and Dutta, A. (2002) *Annu. Rev. Biochem.* **71**, 333–374
- Hashimoto, K., Shimizu, K., Nakashima, N., and Sugino, A. (2003) *Biochemistry* **42**, 14207–14213
- Shcherbakova, P. V., Pavlov, Y. I., Chilkova, O., Rogozin, I. B., Johansson, E., and Kunkel, T. A. (2003) *J. Biol. Chem.* **278**, 43770–43780
- Shimizu, K., Hashimoto, K., Kirchner, J. M., Nakai, W., Nishikawa, H., Resnick, M. A., and Sugino, A. (2002) *J. Biol. Chem.* **277**, 37422–37429
- Prelich, G., Tan, C. K., Kostura, M., Mathews, M. B., So, A. G., Downey, K. M., and Stillman, B. (1987) *Nature* **326**, 517–520
- Lee, S. H., Pan, Z. Q., Kwong, A. D., Burgers, P. M., and Hurwitz, J. (1991) *J. Biol. Chem.* **266**, 22707–22717
- Podust, V., Mikhailov, V., Georgaki, A., and Hubscher, U. (1992) *Chromosoma* **102**, S133–S141
- Schaaper, R. M. (1993) *J. Biol. Chem.* **268**, 23762–23765
- Shinkai, A., Patel, P. H., and Loeb, L. A. (2001) *J. Biol. Chem.* **276**, 18836–18842
- Suzuki, M., Avicola, A. K., Hood, L., and Loeb, L. A. (1997) *J. Biol. Chem.* **272**, 11228–11235
- Suzuki, M., Baskin, D., Hood, L., and Loeb, L. A. (1996) *Proc. Natl. Acad. Sci. U. S. A.* **93**, 9670–9675
- Patel, P. H., Kawate, H., Adman, E., Ashbach, M., and Loeb, L. A. (2001) *J. Biol. Chem.* **276**, 5044–5051
- Minnick, D. T., Bebenek, K., Osheroff, W. P., Turner, R. M., Jr., Astatke, M., Liu, L., Kunkel, T. A., and Joyce, C. M. (1999) *J. Biol. Chem.* **274**, 3067–3075
- Polesky, A. H., Steitz, T. A., Grindley, N. D., and Joyce, C. M. (1990) *J. Biol. Chem.* **265**, 14579–14591
- Dong, Q., Copeland, W. C., and Wang, T. S. (1993) *J. Biol. Chem.* **268**, 24175–24182
- Dong, Q., Copeland, W. C., and Wang, T. S. (1993) *J. Biol. Chem.* **268**, 24163–24174
- Niimi, A., Limsirichaikul, S., Yoshida, S., Iwai, S., Masutani, C., Hanaoka, F., Kool, E. T., Nishiyama, Y., and Suzuki, M. (2004) *Mol. Cell Biol.* **24**, 2734–2746
- Reha-Krantz, L. J., and Nonay, R. L. (1994) *J. Biol. Chem.* **269**, 5635–5643
- Patel, P. H., and Loeb, L. A. (2000) *J. Biol. Chem.* **275**, 40266–40272
- Astatke, M., Ng, K., Grindley, N. D., and Joyce, C. M. (1998) *Proc. Natl. Acad. Sci. U. S. A.* **95**, 3402–3407
- Araki, H., Ropp, P. A., Johnson, A. L., Johnston, L. H., Morrison, A., and Sugino, A. (1992) *EMBO J.* **11**, 733–740
- Patel, P. H., and Loeb, L. A. (2000) *Proc. Natl. Acad. Sci. U. S. A.* **97**, 5095–5100
- Joyce, C. M., and Steitz, T. A. (1995) *J. Bacteriol.* **177**, 6321–6329
- Sambrook, J., and Russell, D. W. (2001) *Molecular Cloning: A Laboratory Manual*, 3rd Ed., Cold Spring Harbor Laboratory, Cold Spring Harbor, NY
- Burke, D., Dawson, D., and Stearns, T. (2000) *Methods in Yeast Genetics: A Cold Spring Harbor Laboratory Course Manual*, Cold Spring Harbor Laboratory, Cold Spring Harbor, NY
- Simon, M., Giot, L., and Faye, G. (1991) *EMBO J.* **10**, 2165–2170
- Lea, D. E., and Coulson, C. A. (1948) *Genetics* **49**, 248–264
- Rosenkranz, H. S., and Levy, J. A. (1965) *Biochim. Biophys. Acta* **95**, 181–183
- Morrison, A., Johnson, A. L., Johnston, L. H., and Sugino, A. (1993) *EMBO J.* **12**, 1467–1473
- Tercero, J. A., and Duffie, J. F. (2001) *Nature* **412**, 553–557
- Singer, B., and Grunberger, D. (1983) *Molecular Biology of Mutagens and Carcinogens*, Plenum Press, New York
- Blank, A., Kim, B., and Loeb, L. A. (1994) *Proc. Natl. Acad. Sci. U. S. A.* **91**, 9047–9051

Yeast Pol δ Leu⁶¹² Substitutions Induce Mutator Phenotypes

36. Holmes, A. M., and Haber, J. E. (1999) *Cell* **96**, 415–424
37. Kokoska, R. J., Stefanovic, L., De Mai, J., and Petes, T. D. (2000) *Mol. Cell Biol.* **20**, 7490–7504
38. Pavlov, Y. I., Shcherbakova, P. V., and Kunkel, T. A. (2001) *Genetics* **159**, 47–64
39. Datta, A., Schmeits, J. L., Amin, N. S., Lau, P. J., Myung, K., and Kolodner, R. D. (2000) *Mol. Cell* **6**, 593–603
40. Zhou, Z., and Elledge, S. J. (1992) *Genetics* **131**, 851–866
41. Shinkai, A., and Loeb, L. A. (2001) *J. Biol. Chem.* **276**, 46759–46764
42. Reha-Krantz, L. J. (1995) *Methods Enzymol.* **262**, 323–331
43. Morrison, A., and Sugino, A. (1994) *Mol. Gen. Genet.* **242**, 289–296
44. Li, L., Murphy, K. M., Kanevets, U., and Reha-Krantz, L. J. (2005) *Genetics* **170**, 569–580
45. Tran, H. T., Keen, J. D., Krickler, M., Resnick, M. A., and Gordenin, D. A. (1997) *Mol. Cell Biol.* **17**, 2859–2865
46. Cariello, N. F., Piegorsch, W. W., Adams, W. T., and Skopek, T. R. (1994) *Carcinogenesis* **15**, 2281–2285
47. Weinert, T. A., Kiser, G. L., and Hartwell, L. H. (1994) *Genes Dev.* **8**, 652–665
48. Gardner, R., Putnam, C. W., and Weinert, T. (1999) *EMBO J.* **18**, 3173–3185
49. Perrino, F. W., and Loeb, L. A. (1989) *J. Biol. Chem.* **264**, 2898–2905
50. Lopes, M., Cotta-Ramusino, C., Pelliccioli, A., Liberi, G., Plevani, P., Muzi-Falconi, M., Newlon, C. S., and Foiani, M. (2001) *Nature* **412**, 557–561
51. Tercero, J. A., Longhese, M. P., and Duffle, J. F. (2003) *Mol. Cell* **11**, 1323–1336
52. Kool, E. T. (2001) *Annu. Rev. Biophys. Biomol. Struct.* **30**, 1–22
53. Kunkel, T. A., and Bebenek, K. (2000) *Annu. Rev. Biochem.* **69**, 497–529
54. Wang, J., Sattar, A. K., Wang, C. C., Karam, J. D., Konigsberg, W. H., and Steitz, T. A. (1997) *Cell* **89**, 1087–1099
55. Franklin, M. C., Wang, J., and Steitz, T. A. (2001) *Cell* **105**, 657–667
56. Goldsby, R. E., Lawrence, N. A., Hays, L. E., Olmsted, E. A., Chen, X., Singh, M., and Preston, B. D. (2001) *Nat. Med.* **7**, 638–639
57. Goldsby, R. E., Hays, L. E., Chen, X., Olmsted, E. A., Slayton, W. B., Spangrude, G. J., and Preston, B. D. (2002) *Proc. Natl. Acad. Sci. U. S. A.* **99**, 15560–15565